CHIN. PHYS. LETT. Vol. 31, No. 8 (2014) 080503

Dynamics of the Kuramoto Model with Bimodal Frequency Distribution on Complex Networks *

FENG Yue-E(冯月娥), LI Hai-Hong(李海红), YANG Jun-Zhong(杨俊忠)**

School of Science, Beijing University of Posts and Telecommunications, Beijing 100876

(Received 9 May 2014)

We introduce a piecewise uniform frequency distribution to model a symmetrical bimodal natural frequency distribution and investigate the dynamics in the Kuramoto model on complex networks. We find that the scenario of the synchronization transition depends on the network topology. For an ER network, the incoherent state, standing wave states and stationary synchronous states are encountered successively with the increase of the coupling strength. However, for an SF network, there exists another type of synchronous states, traveling wave states, between the standing wave states and the stationary synchronous states.

PACS: 05.45.Xt, 89.75.−k DOI: 10.1088/0256-307X/31/8/080503

Synchronization is ubiquitous in physical systems, biological systems, chemical systems, technological systems and social systems.[1−6] A powerful approach on analyzing synchronization in these systems is to model elementary units as phase oscillators when the interaction among them is weak.[7,8] Along this line, Kuramoto worked out a mathematically tractable model, Kuramoto model (KM), which consists of N phase oscillators globally coupled together. Each oscillator has its own natural frequency ω drawn from a given probability density $g(\omega)$ and interacts with the mean field with a global coupling strength λ. For a Kuramoto model, the coupled phase oscillators transit from an incoherent state to a partial synchronization when the coupling strength increases. At the stronger coupling strength, the global synchronization can be built. The theoretical analysis shows that, if $g(\omega)$ follows a bimodal distribution density, there exist standing wave states consisting of two synchronized clusters with different average frequencies[9,10] after the incoherent becomes unstable. Further increasing the coupling strength leads to the transition from the standing wave states to partially synchronous states with a unique synchronous cluster.

Recently, the KM on complex networks in which each phase oscillator only interacts with its nearest neighbors has drawn a great deal of attention.[11] It has also been found that the topological properties of complex networks have strong impacts on the scenarios of the transition to synchronization.[12−15] However, $g(\omega)$ in these works is always a unimodal one. Now it is interesting to investigate how the network topology impacts on the synchronization dynamics when $g(\omega)$ takes a bimodal probability density. Since it is possible that certain characteristic frequencies which are taken by a large fraction of oscillators do not exist, we consider in this work a piecewise probability density $g(\omega)$ with zero mean frequency which consists of two parts and each part is modeled by a uniform probability density.

We start with the KM of N phase oscillators on complex networks

$$\dot{\theta}_i = \omega_i + \lambda \sum_{j=1}^{N} A_{ij} \sin(\theta_j - \theta_i), \ i = 1, \ldots, N, \quad (1)$$

where θ_i and ω_i are the phase and the natural frequency of oscillator i, respectively, λ denotes the coupling strength, $\boldsymbol{A}$ denotes the adjacency matrix of the interaction network, where $A_{ij} = 1$ if oscillators i and j interact with each other, and $A_{ij} = 0$ otherwise. The probability density $g(\omega)$ takes the form

$$g(\omega) = \begin{cases} \frac{1}{2} & \text{if } \omega \in [\frac{\Delta}{2}, 1 + \frac{\Delta}{2}], \\ \frac{1}{2} & \text{if } \omega \in [-1 - \frac{\Delta}{2}, -\frac{\Delta}{2}], \\ 0 & \text{otherwise.} \end{cases} \quad (2)$$

In a more physical interpretation on the bimodal frequency distribution, oscillators are evenly divided into two subpopulations: the positive group (denoted by $+$) consisting of oscillators with positive natural frequencies and the negative group (denoted by $-$) consisting of those with negative natural frequencies. The positive constant Δ represents the detuning of the two subpopulations.

The synchronization in the model Eq. (1) can be described by a global order parameter Z defined as

$$Z = r(t)e^{i\Psi(t)} = \frac{1}{N} \sum_{j=1}^{N} e^{i\theta_j(t)}, \quad (3)$$

where the amplitude r represents the phase coherence, Ψ accounts for the average phase of the system, $r = 0$ represents the incoherent state while $r = 1$ for the global synchronization. We study the dynamics in model Eq. (1) on both scale free networks (SFN) and

*Supported by the National Natural Science Foundation of China under Grant No 71301012.

**Corresponding author. Email: jzyang@bupt.edu.cn

© 2014 Chinese Physical Society and IOP Publishing Ltd

Erdös–Rényi networks (ERN) generated according to Ref. [16] and the model with $N = 1000$ is simulated by using a 4th-order Runge–Kutta method.

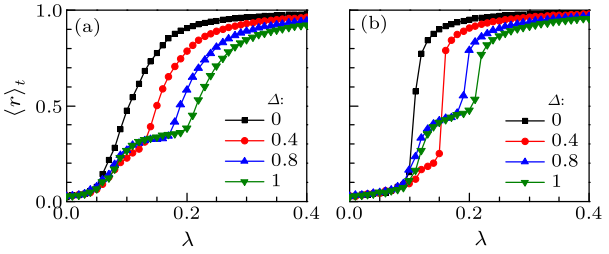


Fig. 1. (Color online) The synchronization diagrams $\langle r(\lambda)\rangle_t$ for a KM on (a) SFN and (b) ERN. The colored symbols stand for different Δ. Here $N = 1000$ and $\langle k\rangle = 12$.

To investigate the synchronization transition in the model Eq. (1), we have computed $\langle r\rangle_t$ as a function of the coupling strength λ where $\langle\cdot\rangle_t$ means the average over a long time interval after transient. In Fig. 1, we show the synchronization diagrams with different Δ for SFN and ERN. In the case of $\Delta = 0$, the amplitude of the order parameter $\langle r\rangle_t$ increases with the coupling strength λ in a continuous way and there exist two different regimes, one for the incoherent states and the other for synchronous states, indicated by the discontinuous change on the slope of $\langle r\rangle_t$ against λ. However, $\langle r\rangle_t$ against λ for $\Delta > 0$ behaves differently. The variation of the slope of $\langle r\rangle_t$ against λ suggests that three parameter regimes exist. The incoherent state ($\langle r\rangle_t \approx 0$) is maintained in the first regime and it becomes unstable in the second and the third regimes. As shown in the following, the synchronous states are different in the second and the third regimes. The critical coupling strength at the transition between these two synchronous states depends on Δ and, generally, it increases with Δ.

To characterize the synchronous states in the second and the third regimes, we introduce local order parameters for the two subpopulations $Z_\pm = r_\pm(t)e^{i\Psi_\pm(t)} = \frac{1}{N_\pm}\sum_{j\in S_\pm} e^{i\theta_j(t)}$, where S_+ (or S_-) represents the positive (or the negative) group and $N_\pm = N/2$. As shown in Figs. 2(a) and 2(b) where $\Delta = 4$, the behaviors of $\langle r_\pm\rangle_t$ against λ become much more complicated. Though $\langle r_\pm\rangle_t$ increases with λ in the third regime, they do not monotonically depend on λ in the second regime. Especially for the SFN, one of $\langle r_\pm\rangle_t$ may decrease when the other increases, which suggests more dynamical behaviors.

To further explore the dynamics in the second and the third regimes, we monitor the time evolutions of Z and $Z_\pm$. The middle (or the bottom) panel (Figs. 2(c) and 2(d) for SFN while Figs. 2(e) and 2(f) for ERN) show the evolutions of r and $r_\pm$ (or Ψ and $\Psi_\pm$). In summary, Fig. 2 shows that there are several types of synchronous states. First, for the synchronous states shown in Figs. 2(c) and 2(e), both the amplitudes and the average phases of the order parameters are time-periodic. Especially, the average phases in the positive and the negative groups oscillate at different frequencies. Secondly, for the synchronous states shown in Fig. 2(d) where the network is an SFN, r and $r_\pm$ become time-independent asymptotically while the average phases are still periodic in time. Especially, three average phases oscillate at the same frequency. Thirdly, for the synchronous states shown in Fig. 2(f) where the network is an ERN, the order parameters are independent of time. Actually, this type of synchronous state is maintained in the whole third parameter regime no matter whether the network is ERN or SFN.

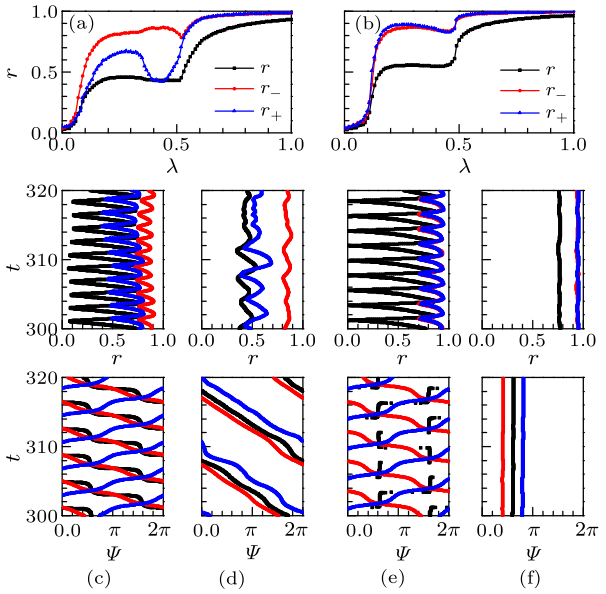


Fig. 2. (Color online) The phase coherence r (in black), r_- (in red), r_+ (in blue) against λ for SFN (a) and for ERN (b). The time evolutions of r (in black), r_- (in red), r_+ (in blue) are plotted in the middle panel and the time evolutions of average phases Ψ (in black), Ψ_- (in red), Ψ_+ (in blue) are plotted in the bottom panel: (c) $\lambda = 0.34$ (SFN); (d) $\lambda = 0.49$ (SFN); (e) $\lambda = 0.37$ (ERN); (f) $\lambda = 0.50$ (ERN). Here $N = 1000$, $\langle k\rangle = 12$, and $\Delta = 4$.

The different synchronous states can be further characterized by investigating the evolution of the phase distribution of oscillators. We consider the phase distributions $P(\theta)$ in the whole population and $P_\pm(\theta)$ in the positive and the negative groups. The evolutions of these phase distributions are presented in Fig. 3 where the parameters and the network topologies are the same as those in Figs. 2(c)–2(f). Clearly, for the synchronous states with periodic phase coherence and periodic average phase, there exist two traveling waves propagating in opposite directions along the phase space (see Figs. 3(a) and 3(c)). Therefore, the synchronous states amount to the standing wave states. On the other hand, Fig. 3(b) suggests that the synchronous states with time-independent phase co-

herence and time-periodic average phases represent traveling wave states where all phase distributions travel along the phase space at the same velocity. Figure 3(d) shows that the states in Fig. 2(f) amount to stationary synchronous ones in which the phase distributions are motionless in the phase space. To be stressed, in comparison with the original KM with symmetrical bimodal frequency distribution, the KM on complex networks with the frequency distribution following Eq. (2) displays another type of synchronous states, the traveling wave states, in addition to the standing wave states and the stationary synchronous states.

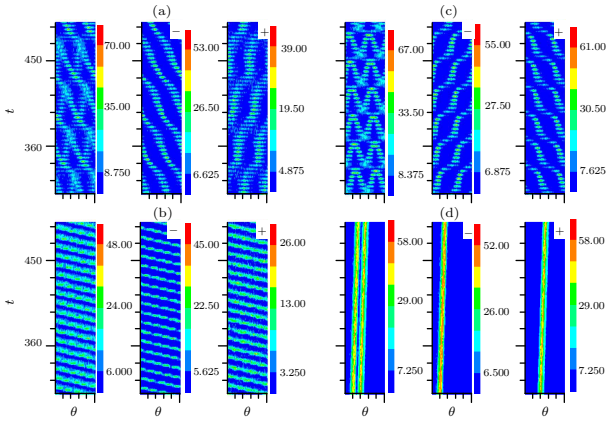


Fig. 3. (Color online) The time evolutions of the phase distributions at different coupling strengths: (a) $\lambda = 0.34$ (SFN), (b) $\lambda = 0.49$ (SFN), (c) $\lambda = 0.37$ (ERN), (d) $\lambda = 0.50$ (ERN). The parameters are the same as those in Figs. 2(c)–2(f).

To understand the nonmonotonic dependence of $r_\pm$ on λ, we compute the effective frequency for every oscillator, which is defined as $\omega_e = \langle \frac{d\theta}{dt} \rangle_t$. To better figure out the organization of oscillators during the synchronization transition, we sort oscillators according to their effective frequencies and their natural frequencies. The first $N/2$ indices belong to the negative group and the others to the positive group. On the other hand, we have $i < j$ if $\omega_e(i) < \omega_e(j)$.

The top panel in Fig. 4 shows the results for the KM on an SFN. When the coupling strength is slightly above the onset of synchronization, the effective frequencies in the negative and the positive groups are disconnected and the graph of $\omega_e(i)$ shows two plateaus at different effective frequencies (see Fig. 4(a) with $\lambda = 0.07$), which indicates the formation of synchronous clusters in the negative and the positive groups. Different from the globally coupled KM with bimodal symmetrical $g(\omega)$ where two plateaus are always symmetrical, here the plateaus in the positive and the negative groups are asymmetrical. Generally, increasing the coupling strength always expands the plateaus on the graph $\omega_e(i)$ and reduces the difference between the effective frequencies of the plateaus for a globally coupled KM. However, for the KM on an SFN with a symmetrical frequency distribution, with the increases of λ, one of the plateaus on the graph $\omega_e(i)$ may be reduced while the other is expanding (see Fig. 4(b) with $\lambda = 0.37$). Consequently, one of the plateaus could be eaten up as shown in Fig. 4(c) where only one plateau at nonzero effective frequency remains. At a sufficiently strong coupling strength, the plateau on the graph $\omega_e(i)$ shifts to the one at zero effective frequency and becomes symmetrical about $i = N/2$. The bottom panel in Fig. 4 shows the results for the KM on an ERN. Different from the case with the SF network, the plateaus on the graph $\omega_e(i)$ are always symmetrical about $\omega_e = 0$.

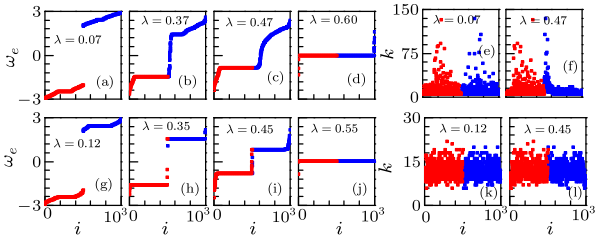


Fig. 4. (Color online) The graph of the effective frequencies $\omega_e(i)$ and the degree of oscillators $k(i)$ are plotted, where i is the index of oscillators sorted according to their effective frequencies and natural frequencies. The top panel shows the graph for SFN: (a)–(d) for the graph of $\omega_e(i)$; (e, f) for the graph of $k(i)$. The bottom panel shows the graph for ERN: (g)–(j) for the graph of $\omega_e(i)$; (k, l) for the graph of $k(i)$. The oscillators in the positive group are denoted in blue and the oscillators in the negative group in red.

In Fig. 4, we find that oscillators with positive (or negative) natural frequencies may be trapped by the negative (or the positive) group (see Figs. 4(b) and 4(c) for SFN and Figs. 4(h) and 4(i) for ERN). Since $r_\pm$ represents the phase coherence in the positive and the negative groups, such an observation in Figs. 4(a)–4(c), and Figs. 4(g)–4(i) actually present the explanations on the nonmonotonic dependence of $r_\pm$ on λ. Actually, the phenomenon roots in the fact that oscillators only interact with their neighbors. For example, the oscillators with positive natural frequencies tend to be trapped by the negative group if they are neighboring the synchronous cluster in the negative group.

The observation that the traveling wave states on SFN while not on ERN can be explained by different scenarios of synchronization transition on these two types of networks. As claimed in Ref. [15] where a KM with unimodal frequency distribution is studied, the synchronization transition on an SFN starts with a synchronous cluster centering a hub with high degree. Then the synchronous cluster grows by recruiting its neighbors till the global synchronization is reached. On the other hand, in the synchronization transition on an ERN, there exist many synchronous clusters and the global synchronization is approached through the merger of these clusters. For a KM with

bimodal frequency distribution on an SFN, there may be two synchronous clusters centering at the hubs, one for the positive group and the other for the negative group (see Figs. 4(e) and 4(f)). Though the natural frequency distribution of oscillators is symmetrical, the degree heterogeneity and the random assignment of oscillators onto the network render one of the synchronous clusters dominant. At the strong coupling strength, the dominant synchronous cluster may trap all oscillators in the other one and, consequently, the traveling wave states are realized. On the other hand, for a KM with bimodal frequency distribution on an ERN, there are many synchronous clusters that have no preference on degree (see Figs. 4(k) and 4(l)), which means that neither the positive group nor the negative group can be the dominant one due to the random assignment of oscillators onto the network. As a result, we always observe symmetrical plateaus on the graph $\omega_e(i)$ for ERN.

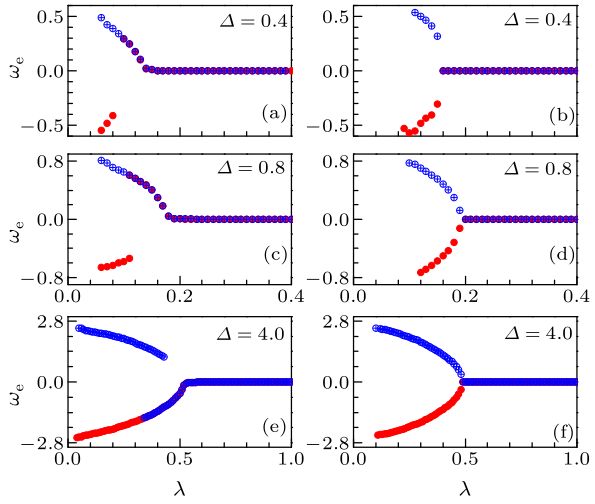


Fig. 5. (Color online) The effective frequencies ω_e of the plateaus are plotted against the coupling strength λ for different Δ (the red symbols for the negative group and the blue symbols for the positive group). The left column is for SF networks and the right column for ER networks.

To obtain an overview on the model Eq. (1) with Eq. (2), we present the effective frequencies of plateaus against the coupling strength for different Δ. The left column in Fig. 5 shows that the incoherence states, the standing wave states, the traveling wave states, and the stationary synchronous states are experienced successively with the increase of λ on SF networks. On the other hand, the right column in Fig. 5 shows the absence of the traveling wave states on ER networks. The buildup of the stationary synchronous states is induced by the mutual synchronization between the synchronous clusters in the positive and the negative groups.

In conclusion, we have introduced a piecewise uniform frequency distribution which is symmetrical about $\omega = 0$ and investigated the KM on complex networks. Different scenarios on synchronization transition on complex networks are found. It is realized that the KM on ER networks behaves like a globally coupled one. During the synchronization transition, the incoherent state, standing wave states and the stationary synchronous states appear successively with the increase of the coupling strength. On the other hand, the KM on SF networks behave differently. There exist traveling wave states between the standing wave states and the stationary synchronous states.

It is well known that the network structures are time-dependent in the real world.[17,18] It is worth mentioning that the observations in this work can be found in a KM on time-varying networks.

References

[1] Winfree A T 1980 *The Geometry of Biological Time* (New York: Springer)
[2] Strogatz S H 2003 *sync: The Emerging Science of Spontaneous Order* (New York: Hyperion)
[3] Neda Z, Ravasz E, Vicsek T, Brechet Y and Barabasi A L 2000 *Phys. Rev.* E **61** 6987
[4] Guo X Y and Li J M 2011 *Chin. Phys. Lett.* **28** 120503
[5] Eckhardt B, Ott E, Strogatz S H, Abrams D M and McRobie A 2007 *Phys. Rev.* E **75** 021110
[6] Wei D Q, Luo X S, Chen H B and Zhang B 2011 *Chin. Phys. Lett.* **28** 110501
[7] Strogatz S H 2000 *Physica* D **143** 1
[8] Acebrón J A, Bonilla L L, Pérez-Vicente C J, Ritort F and Spigler R 2005 *Rev. Mod. Phys.* **77** 137
[9] Kuramoto Y 1984 *Chemical Oscillations, Waves and Turbulence* (New York: Springer)
[10] Martens E A, Barreto E, Strogatz S H, Ott E, So P and Antonsen T M 2009 *Phys. Rev.* E **79** 026204
[11] Hassan F E N, Paulsamy M, Fernando F F and Cerdeira H A 2009 *Chaos* **19** 013103
[12] Moreno Y and Pacheco A F 2004 *Europhys. Lett.* **68** 603
[13] Arenas A, Díaz-Guilera A and Perez-Vicente C J 2006 *Phys. Rev. Lett.* **96** 114102
[14] Zhou C S and Kurths J 2006 *Chaos* **16** 015104
[15] Gómez-Gardeñes J, Moreno Y and Arenas A 2007 *Phys. Rev. Lett.* **98** 034101
[16] Gómez-Gardeñes J and Moreno Y 2006 *Phys. Rev.* E **73** 056124
[17] Chen Y, Lü J H, Yu X H and Lin Z L 2013 *SIAM J. Control Optim.* **51** 3274
[18] Lü J H and Chen G R 2005 *IEEE Trans. Autom. Control* **50** 841